Estimation of the main fluid flow parameters of strombolian eruptions from acoustic measurements

Juan José Peña Fernández, Jörn Sesterhenn
Institut für Strömungsmechanik und Technische Akustik, 10623 Berlin, Deutschland, Email: fernand@tnt.tu-berlin.de

Abstract

The same way that we can hear that the wind is blowing faster or slower, we can hear when pouring water from a teapot that the water is hot, due to the coupling between fluid mechanics and acoustics. In volcanology we do not have direct access to the fluid flow, so we look for another way to estimate the magnitudes we are interested in. The objective is to estimate the four main fluid flow parameters of real eruptions (nozzle pressure ratio (NPR), non-dimensional mass supply (L/D), Reynolds number (Re) and temperature ratio (T_r/T_∞)) from acoustic measurements. More than 10 000 eruptions have been recorded at the Mount Etna and Stromboli with an array of 3 microphones to have the noise radiated in different directions. The governing parameters were estimated using existing correlations in the literature. Good agreement has been found between the acoustics radiated from the numerical simulations and the acoustics measured at the Mount Etna. Acoustic measurements of real eruptions were carried out estimating the governing parameters with the help of correlations from the literature. Numerical simulations of a starting free jet were performed and the radiated acoustics had a good agreement with the measured at the volcanoes.

Introduction

In volcanology, as well as in many other practical applications either the direct access to the fluid flow is not possible, or the act of measuring includes unacceptable errors in the measurements due to disturbances of the fluid flow created intrinsically by the act of measuring. With this motivation the objective of this work is to estimate the governing parameters of the starting jet from acoustic measurements, without disturbing the flow field and from a safety place.

To this end, we found the governing parameters of the starting jet and we linked the physical phenomena of the starting jet and their acoustics by means of a direct numerical simulation.

The numerical simulation was performed using an in-house numerical code discretising the compressible Navier-Stokes equations in the characteristic form as in [1] using 6^{th} order finite differences for the spatial discretisation and 4^{th} order Runge-Kutta for the time integration method. The grid used had $2048 \times 1024 \times 1024$ grid-points in $x-$, $y-$, and $z-$ directions, respectively, discretising a box of $25 \times 15 \times 15$ nozzle diameters in the three directions, respectively. More details are given in [2, submitted].

After coupling the fluid mechanics with the acoustics of the starting jet, we estimated the governing parameters of the starting jet from acoustic measurements in a theoretical framework.

In this work we applied the developed method to real volcanic eruptions, that we measured at the mount Etna and Stromboli and we estimated the main flow parameters in order to monitor in real time the state of the volcano.

The present work is organised as follows: in the following subsections of this section the elements of the starting jet are described together with the acoustics. The next section describes and discusses the results obtained in this work showing the typical sound pressure level spectra obtained from the real eruption measurements and the last section of this work concludes it and puts it into the proper context.

Elements of the Starting jet

Figure 1 shows the main elements of the starting jet for the different stages of the whole process to see their temporal evolution.

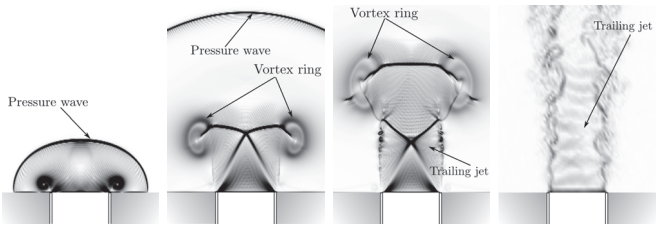

(a) Pressure wave (b) Vortex ring (c) Trailing jet (d) Decay

Figure 1: Main elements of the starting jet. (a) Pressure wave and the initial state of the vortex ring. (b) Pressure wave for a later time and a developed vortex ring. (c) Vortex ring with a shock-wave in its interior and the first stage of the trailing jet. (d) Subsonic trailing jet during the decay stage.

Just after the release of the pressure at the reservoir, the first pressure wave travels in all directions of the space after the nozzle with the speed of sound. With the beginning of the movement at the lip of the nozzle, the vortex ring is created and fed with vorticity.

The longer and the faster is the movement, the stronger is the vortex ring. However, there is a limiting value for the non-dimensional mass supply that defines the existence of the trailing jet. This limiting value was stated for the first time in [3] with the value $(L/D)_{\text{lim}} \sim 4$ and

later corrected by several authors to be dependent of different parameters like the time distribution of the inlet condition and the Reynolds number to reach values between 1 and 5. There will exist a trailing jet only if the non-dimensional mass supply is larger than this limiting value $(L/D)_{\mathrm{lim}}$.

Depending on the pressure ratio, the trailing jet and the vortex ring will be subsonic or supersonic. In case of being subsonic the trailing jet will only have a shear layer. In the supersonic case it will have as well shock-waves, which will affect drastically the acoustic footprint of the whole process.

The final stage of the jet is typically characterised by a decay. During this stage the velocities decay to zero and all the thermodynamical variables decay to the state of quiescence.

Acoustics of the Starting jet

The main jet acoustic components of the starting jet are the three classic ones of the continuous jet (the turbulent mixing noise, the broadband shock noise and the screech), and the ones due to the starting stage, which are the first pressure wave and the corresponding to the vortex ring.

The **first pressure wave** acoustics are due to its arrival to the sensor/listener, being a single pressure wave with a semi-spherical shape propagating into the surroundings of the nozzle.

The **vortex ring** acoustics can be separated into the turbulent and laminar case; the former is much louder than the latter, being in both cases the main sound radiation in the perpendicular direction of the jet axis.

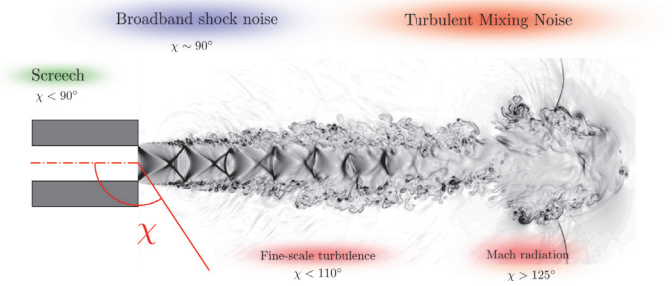

Figure 2: Jet noise directivity. While screech tones are mainly radiated backwards, the turbulent mixing noise is mainly radiated in the downstream direction, being the large-scale turbulent acoustics radiated for $\chi > 125°$ and the fine-scale turbulent acoustics for $\chi < 110°$. The broadband shock noise is radiated in the normal direction to the jet axis.

The directivity of the typical noise components of the continuous jet have been already reported in the literature [4, 5, 6], being summarised in the figure 2 and in the following: the screech tone is mainly radiated in the rear arc, while the broadband shock noise is radiated in the angles almost normal to the jet axis. The turbulent mixing noise is mainly radiated downstream, differentiating the fine-scale turbulence in the angles $\chi < 110°$ from the large-scale turbulence in the angles $\chi > 125°$.

Estimation of the main flow parameters

As it was first stated in [7], the peak Strouhal number for the fine-scale similarity spectrum increases with increasing Reynolds number so, that measuring its peak Strouhal number we can read the Reynolds number. In this way, taking into account the extended database available at the moment (and even extended by our group through numerical simulations as well as experiments), we can estimate the Reynolds number.

The same way, the NPR can be estimated through the sound pressure level of the large-scale similarity spectrum as first stated by [4], in which the temperature ratio was also taken into account, being able to estimate T_r/T_∞ the way it is described in [2, submitted].

In the case the flow is supersonic, the nozzle pressure level can also be estimated by the peak Strouhal number of the broadband shock noise, due to the different shock-cell lengths with the Mach number generated by increasing the NPR.

Once the rest of the parameters are already estimated, we can assume the system discharges fluid from a reservoir, we can assume a typical pressure time profile at the inlet and in this way we can estimate the non-dimensional mass supply L/D as described in [2, submitted].

Typical sound pressure level spectra

In this section we show and discuss single sound pressure level spectra measured at the mount Etna and Stromboli. We have chosen 4 cases that cover the whole phenomenology. For the sake of clearness we start with the case with only one physical phenomenon and we increase the complexity of the phenomenology for the following cases.

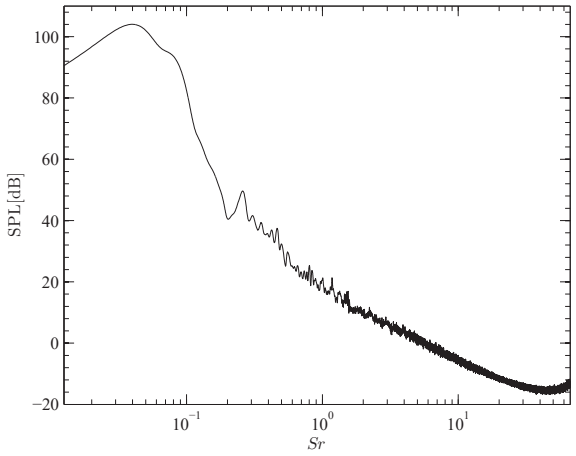

Figure 3: Typical sound pressure level for an eruption in which only a pressure wave is radiated.

For a very short eruption, a **pressure wave** is radiated in the surroundings together with a laminar vortex ring (which does not radiate any acoustic). A measured spectrum of this kind is shown in figure 3. This is the basic

setup for the acoustic measurements, in which we notice the different damping over the frequency spectrum of the pressure wave.

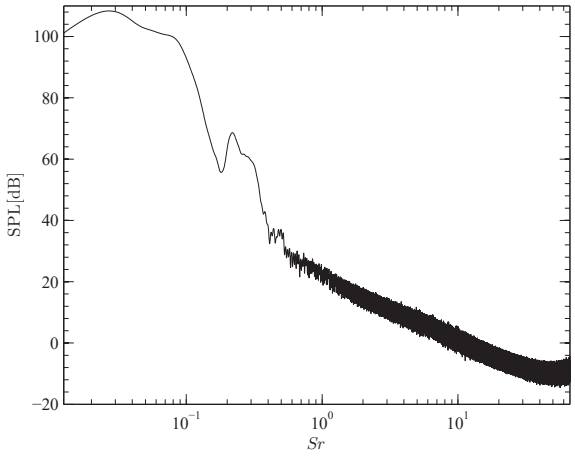

Figure 4: Typical sound pressure level for an eruption in which a pressure wave is radiated together with a vortex ring, but without any trailing jet.

The next step is to add the effect of the **vortex ring acoustics** to the previous configuration, which means physically that the vortex ring has become turbulent and therefore contributes to the acoustics. This case is shown in figure 4. The difference with the previous case is the peak at $Sr \sim 0.25$ giving also very important information about the size of the vortex ring.

When the eruption blows for a longer time (when the non-dimensional mass supply L/D is larger), the starting jet has a trailing jet, which also contributes to the acoustics in the surroundings. In this case both the **turbulent mixing noise** and the **broadband shock noise** can be seen in figure 5. The black curve corresponds to the spectrum calculated from the whole eruption, in which there is a supersonic stage and a subsonic one (during the decay), while the grey curve corresponds to the spectrum calculated only from the subsonic stage, taking a small time window during the decay stage. Both curves are qualitatively different; the black curve shows the turbulent mixing noise for low frequencies, but the broadband shock noise for Strouhal numbers from $Sr \sim 0.4$ on. The grey curve shows only turbulent mixing noise, since it was taken from the purely subsonic flow during the decay phase.

For a long enough eruption to have a supersonic trailing jet, but short enough not to radiate the whole spectrum of the broadband shock noise, only the higher frequencies of it will be radiated as shown in figure 6. In this way we can also estimate the length of the supersonic stage, by taking into consideration the lowest frequency radiated by the broadband shock noise.

The **screech tone** was not present neither in the measurements nor in the simulations, and it was out of the scope of this study, and therefore was not investigated, but the frequency of the screech tone is also a good indicator of the Mach number of the flow, and we can therefore estimate the NPR from its frequency.

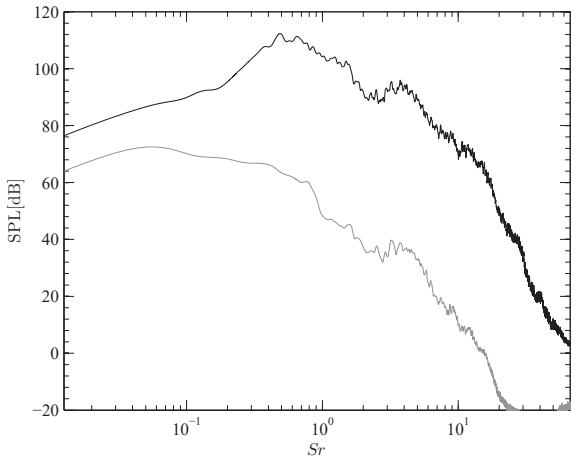

Figure 5: Typical sound pressure level for a starting jet with all components. In black is the spectrum for the whole eruption. In grey, the subsonic final part of the eruption when the velocities are in the decay stage.

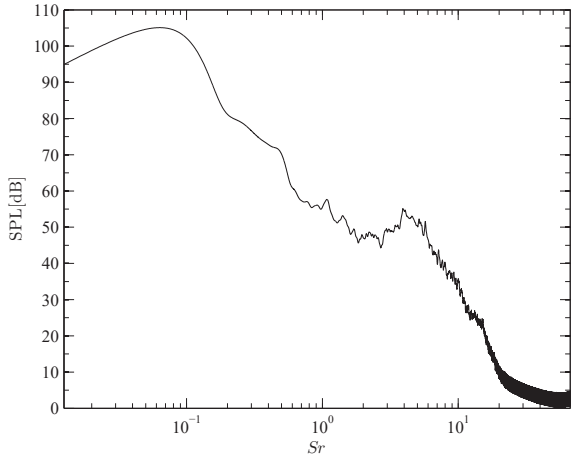

Figure 6: Typical sound pressure level for an eruption in which a pressure wave is radiated together with a vortex ring and a supersonic trailing jet for a short period of time.

For an eruption in which the flow is supersonic, the turbulent mixing noise will not be visible in the spectrum when taking into consideration the whole eruption, but taking only a time window in which the flow is subsonic, we can measure the turbulent mixing noise and with it we can make the estimation of the corresponding parameters, scaling the pressure due to the decay that has taken place already in this stage of the flow.

Estimated parameters

With the method described in section we estimated the governing parameters of the eruptions measured at the Mount Etna and Stromboli. In the following, the estimation of the four governing parameters (Re, NPR, T_r/T_∞ and L/D) will be presented.

For the Reynolds number, we estimated values in the range $Re = \{10^5 - 10^8\}$, which is a realistic value taking into consideration the big diameter of the craters and the high velocities that take place in the vent.

For the case of the NPR, the estimated values are in the range of NPR$= \{2.3 - 5\}$, which are underestimated. The reason of this is that actually the Mach numbers were estimated and from them the pressure ratio was calculated assuming a steady system. This estimation would be very good for very large reservoirs, but not for small ones. We have to work further in this aspect to improve the results. If we replace the NPR with the fully expanded Mach number M_j we would have had very good results, but this is not an excuse to work further to get the pressure ratio, but a way to define the source of the error.

For the temperature ratio, the estimated values are in the range $T_r/T_\infty = \{3.3 - 4.91\}$, which is a very good estimation, taking into consideration that typical values of the magma temperature are in the range from 800 to 1200° C.

Concerning the non-dimensional mass supply, the estimated values are in the range $L/D = \{0.5 - 3\}$, which are realistic, indicating the size of the bubbles that arise to the magma surface and lead to the corresponding eruptions. This values are within the typical values for the bubble size of this two volcanoes.

Conclusions

After performing a direct numerical simulation of a compressible starting jet we linked the fluid mechanics with the acoustics in order to estimate the governing parameters from acoustic measurements.

We estimated successfully the governing parameters of the measured eruptions, although the presence of echos and other noise in the signals. The different acoustic components are separated in four typical sound pressure level spectra that represents the whole phenomenology. The four typical sound pressure level spectra have been here discussed.

The estimated values of the governing parameters are realistic and they are within the typical values for the two mentioned volcanoes.

The next step to be done is to work in an interdisciplinary team, measuring a single eruption with several devices, estimating the governing parameters of the eruptions using different methods and comparing the results. Two campaigns are planned in may and october 2016 to this end.

Acknowledgments

The authors gratefully acknowledge the Gauss Centre for Supercomputing e.V. (www.gauss-centre.eu) for funding this project by providing computing time on the GCS Supercomputer SuperMUC at Leibniz Supercomputing Centre (LRZ, www.lrz.de).

References

[1] Sesterhenn, J. 2000. A Characteristic-type formulation of the Navier-Stokes equations for high order upwind schemes. Computers and Fluids. Volume 30. pp. 37-67.

[2] Pena Fernandez, J.J. and Sesterhenn, J. 2016. Compressible starting jet: governing parameters and their estimation from acoustics measurements. Journal of Fluid mechanics. Submitted.

[3] Gharib, M. and Rambod, E and Shariff, K. 1998. A universal time scale for vortex ring formation. Journal of Fluid Mechanics. Volume 360, pp. 121-140.

[4] Tam, C.K.W. and Golewiobski, M. and Seiner, J.M. 1996. On the two components of the turbulent mixing noise from supersonic jets. Aeroacoustics Conference, AIAA Journal.

[5] Tam, C.K.W. 1995. Supersonic jet noise. Annual Review of Fluid Mechanics. Volume 27, pp. 17-43.

[6] Norum, T.D. and Seiner, J.M. 1982. Broadband shock noise from supersonic jets. AIAA Journal. Volume 20, pp 68-73.

[7] Bailly, C. and Bogey, C. 2006. Current understanding of jet-noise generation mechanisms from compressible large-eddy simulations. In Direct and Large Eddy Simulations VI, pp. 39-48. Springer.